

Magnetic Coils for Ultracold Atom Control

Nolan Maloney, Walla Walla University, 2008.

I. The Experiment

A. Introduction

The first Bose-Einstein condensate (BEC) was achieved with rubidium-87 in 1995 by Wieman and Cornell [1], for which they were awarded the Nobel Prize in 2001. This was a confirmation of the predictions made by Bose and Einstein in the early 20th century of this new state of matter, in which most of the bosons condense down into the same state. Since then, ultra-cold atom research with bosons as well as fermions has become an increasingly important area of research in atomic, molecular, and optical physics. It is an area of rapid progress that is certainly one of the most interesting in the field of physics today.

Some of the excitement regarding the study of ultra-cold atoms is rooted in the ability to study the physical properties of these condensates, while having the ability to control the mechanical degrees of freedom and weak interactions. These ideas constantly test and challenge the developing theories that describe their behaviors. There are an increasing number of groups who see new research opportunities in this field and who see applications for the discoveries and developments that are being made. In this paper, we describe the anti-Helmholtz coils for the magneto-optical trap (MOT) and the Helmholtz coils for feshbach resonances used for interaction control.

B. Magneto-Optical Trap and Laser Cooling

These experiments are done under ultra-high vacuum and the first major stage of cooling is done with lasers. The atoms in the atomic beam entering the MOT are initially slowed by Zeeman slower. The basic process is that the absorption and rescattering of photons gives a resulting recoil or slowing “kick.” In the Zeeman slower, the atom beam is directed along the axis of a tapered solenoid in the opposite direction to a resonant laser beam; the Zeeman shift through the varying magnetic field keeps the atoms in tune with the counter-propagating laser. The atoms are now traveling slow enough to be captured in the MOT,

$$v = \frac{\hbar\Gamma}{k_B},$$

where v is the velocity the atoms leave the slower and Γ is the linewidth of the transition [2].

The MOT consists of two coils with currents flowing in opposite directions that produce a quadrupole magnetic field. This creates a magnet field gradient. At the center of the trap the magnetic field is zero. There are three sets of counter-propagating, circularly polarized laser beams that are at a frequency slightly less than that of the atomic resonance (red-detuned). Atoms that drift toward one of the lasers will be brought into resonance with the laser (by the magnetic field – the Zeeman effect), will absorb a photon, and the momentum received from the photon will give the atom a “kick” toward the center of the trap [2].

Breakthroughs in laser cooling brought tremendous progress towards the creation of a BEC, but it has a lower limit. Assuming a two-level atom, the Doppler cooling limit gives the lowest temperature expected for the optical molasses technique and is given by

$$T_D = \frac{\hbar\Gamma}{2k_B}.$$

This is due to the random walk of the atoms from spontaneous absorption and emission of photons. There are additional techniques that allow laser cooling below the Doppler limit, which cannot be explained by the two-level atom. These techniques have a lowest temperature given by the recoil limit,

$$T_r = \frac{\hbar^2 k^2}{k_B M},$$

where M is the mass of the atom being used. Sodium, for example, which has a line width of $2\pi \times 10$ MHz, has a Doppler cooling limit of 240 μ K and a recoil limit of 2.4 μ K. Conditions for the formation of a degenerate gas are that the deBroglie wavelength is on the order of the interparticle spacing, that is, $n\lambda_{dB}^3 \approx 1$. This gives a critical temperature that goes like

$$T_C \approx \frac{1}{k_B} \frac{\hbar^3 \bar{\omega}}{N^3},$$

where N is the number of atoms in the trap and $\bar{\omega}$ is the trap frequency. For a trap with a frequency of $\bar{\omega}=50\text{Hz}$ containing $N \approx 10^6$ atoms, the critical temperature is $T_C \approx 38nK$. Additional cooling is necessary for the formation of a quantum degenerate gas.

C. Evaporative Cooling

The last stage of cooling is done by a process called evaporative cooling. The process is analogous to the evaporative cooling of a cup of coffee or the sweat on your skin. Either the walls of the potential well trapping the atoms can be lowered or the most energetic atoms can be preferentially untrapped (e.g. RF-induced spin-flipping). The most energetic atoms will leave the trap and the atom cloud will be left with a lower average energy. It is necessary to have sufficient collisions in the gas so that rethermalization will occur. This results in a restoration of the Maxwell-Boltzmann distribution at the lower temperature and allows evaporative cooling to continue. There is no fundamental lower limit for evaporative cooling [2].

D. Feshbach Resonance

The strong, homogeneous magnetic field will be used for manipulating the interaction between the particles through Feshbach resonance. At these temperatures, the s-wave scattering length characterizes the interaction between particles. When the energy of the free particles is higher than the bound state, the scattering length is positive and the particles tend to form molecules. When the bound state energy is higher, the scattering length is negative and fermionic particles with opposite spins tend to form long-range, BCS-like pairs. The magnetic field can be used to tune the relative energy levels. At around 834 Gauss for Lithium, the scattering length diverges. Across this transition, the particles change from having a tendency to form molecules to forming long-range pairs [3].

II. The Magnetic Coils

A. Design

Two different magnetic field shapes are desired for this experiment. One field needs to be fairly constant with a low curvature and a low gradient at the center, where the atom cloud would be. This is achieved using a set of coils in a Helmholtz arrangement. Additionally, it is desirable to have a high magnetic field to current ratio for this coil, since it will be necessary to create fields of 800 – 1000 Gauss. This reduces the heating, which is proportional to the square of the current ($P=I^2R$). The other field needs to have a high gradient at the center of

the trap, which can be achieved by placing a set of coils on each side of the trap with current running in opposite directions (anti-Helmholtz). The separation between the anti-Helmholtz coils is not critical like it is for the Helmholtz coils.

Each coil pair will be connected in series in order to ensure an equal amount of current in each coil. Building a separate set of coils for each field requirement gives the flexibility of not having to switch currents configurations in the coils. Together both of these coils needed to fit inside and against the inner face of each recessed vacuum viewport on the apparatus (5.76 inches in diameter), avoiding a 2.73 inch flange its center. A small amount of space needed to be taken into account for the epoxy to hold the coils together. Additionally, it was necessary to construct the coils with an even number of radial turns for each coil so that the leads would both enter and exit from the same side of the coil.

The actual dimensions of the coils were arrived at by calculating magnetic fields in the program Mathematica. The coils were approximated as a sum of current loops (one for each turn on the actual coil), which were correctly spaced according to the wire thickness. Calculation of the magnetic fields due to the current loops was done using the Biot-Savart Law,

$$d\vec{B} = \frac{\mu_0}{4\pi} \frac{I \cdot d\vec{l} \times \hat{r}}{r^2}.$$

The parameters of the coils were adjusted while observing the resulting axial field due to that design.

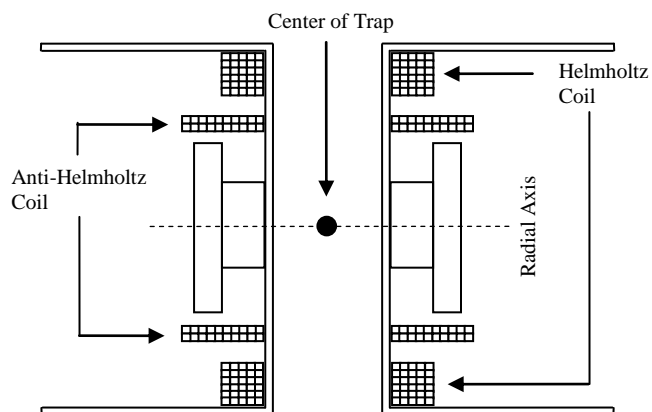


FIG. 1. Recessed vacuum viewports – vertical cross-section (not to scale).

Finalized coil designs were decided upon once the magnetic field properties were optimized and the physical dimensions were within constraints. Each coil pair will be held at a distance of 1.74 inches (from the inside face of one coil to the inside face of the other – a

constraint of the vacuum chamber construction). The design settled on for the Helmholtz coils had an inside diameter of 3.95 inches and an outside diameter of 5.57 inches. It contains 6 radial turns and 5 axial turns (a total of 30 current loops). The outside diameter of this design will come relatively close to the inside diameter of the recessed viewport, but allows for some epoxy on the coils and some minor adjustments in position when placed in the recessed viewport. According to the model, at the center of the trap, the magnetic field should have a strength of 4.4 G/A and a curvature of .009 G/cm²/A. The design for the anti-Helmholtz coils had an inside diameter of 2.95 inches and an outside diameter of 3.49 inches. It contains 2 radial turns, and 10 axial turns (they will be placed similarly in the recessed viewport inside the Helmholtz coils). According to the model, this coil pair should have a gradient of .86 G/cm/A at the center of the trap. The Helmholtz coils should have a resistance of about 24.5 mΩ each at 25°C and the anti-Helmholtz coils should have a resistance of about 11.8 mΩ each (using the length of the coil plus about 20 cm for leads).

B. Construction

For the construction of the coil, kapton coated 1/8 inch, hollow, square copper wire made by Essex was used (the wire was insulated by SW Wire). The hole is 1/16 inch square and is for coolant. The whole wire is approximately .135 inches square including the insulation. This wire was wound by hand on an aluminum mandrel held by a lathe. This aluminum guide was composed of four pieces held together by a half-inch bolt that was tightened, holding the pieces rigid: one piece to be held by the lathe, two pieces to define the two faces of the coil (they guided the wire as it got close to the edges), and the fourth piece in between the edge guides to wind the wire onto (which has an outer diameter equal to the inner diameter of the coil).

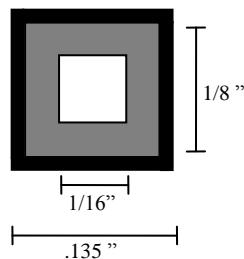


FIG. 2. Copper wire used.

The square wire was passed through a wooden guide (held by the lathe's tool mount), which provided friction for the wire. This kept the coil tightly wound and kept the wire from twisting as it was wound onto the mandrel. Each layer was completely wound before moving radially outward to the next layer.

Once the winding was complete the incoming and outgoing leads, which were left about 3 meters long, were arranged with zip ties to lie next to each other. For rigidity, the whole coil was covered with a thermally conductive epoxy (the Durapot 865 EPOX-EEZ from Cotronics), except for the inside face. This will allow the coils to lie flat against the bottom of the recessed viewport

and to be as close to each other as possible. The chamber can be baked with the coils in place up to 260°C (limited by epoxy).

C. Testing

Testing of the coils was done by mounting them on aluminum plates, which were held at a fixed distance from each other equal to the spacing that they will have in the MOT. A brass tube passed through the center of the plates along the axis of the coils and was used to guide the axial probe (HAD61-2508-05-T) of the Model 6010 Gauss/Tesla-meter (manufactured by Sypris). Measurements were made with a controllable DC current passing through the coils. A dowel with millimeter markings on it was attached to the probe and moved in consistent intervals. The probe had a plastic guide attached to it, which held it centered inside the brass tube. The error in the readings, according to the Gauss/Tesla-meter manual, is .25% of the measured value. This was the most limiting factor in determining the characteristics of the constructed coils.

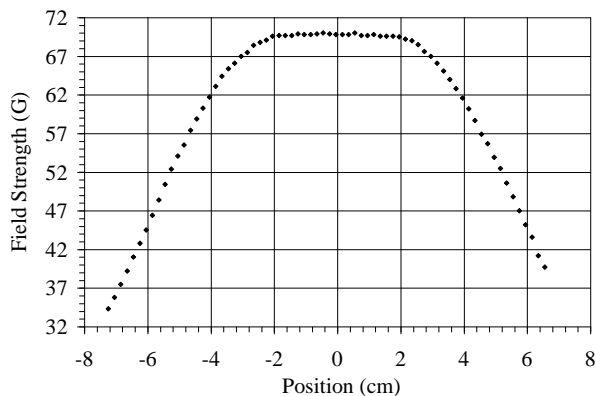


FIG. 3. Helmholtz coils with 16 Amperes of current.

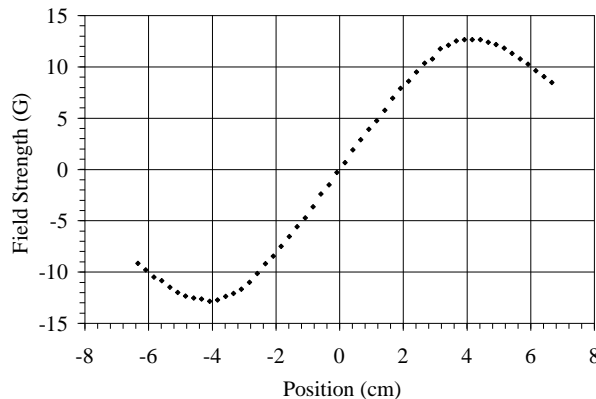


FIG. 4. Anti-Helmholtz coils with 5 Amperes of current.

Fits were made to the data to determine the maximum gradient and curvature of the Helmholtz coils and to determine the gradient of the anti-Helmholtz coils. The Helmholtz coils, which produced a measured field strength of approximately 4.37 G/A, was determined to have an axial curvature of less than .025 G/cm²/A and an axial gradient of less than .013 G/cm/A at the center. The gradient should have been zero, but it appears that one coil is slightly stronger than the other coil. These two factors combine to give a variation of significantly less than 1 Gauss over a distance of 1 mm when the field is at 1000 Gauss. The anti-Helmholtz coils had a measured gradient of about .84 G/cm/A at the center. The resistances of the coils were also measured (plus about 10 cm of wire for each lead). The resistance of the Helmholtz coils is about 26.3 mΩ each and the resistance of the anti-Helmholtz coils is about 12.4 mΩ each.

Actual Dimensions (without epoxy)

	Helmholtz	Anti-Helmholtz
Inside Diameter (cm)	3.95	2.95
Outside Diameter (cm)	5.57	3.49
Radial Turns	6	2
Axial Turns	5	10
Length	.7	1.36

Helmholtz Coils

	Predicted	Measured
Resistance (mΩ) (each)	24.5	26.3
Strength (G/A)	4.4	4.37
Gradient (G/cm/A)	0	<.013
Curvature (G/cm ² /A)	.009	<.025
Inductance (mH)	>.1 (est.)	

Anti-Helmholtz Coils

	Predicted	Measured
Resistance (mΩ) (each)	11.8	12.4
Gradient (G/cm/A)	.86	.84
Inductance (mH)	≈ .03 (est.)	

D. Conclusion

The measurements made for these coil arrangements agree with calculations and indicate that they are adequate for this experiment. Since the values from the worst fits are acceptable, there is confidence that the coils will perform well in the experiment.

[1] M. H. Anderson, J.R. Ensher, M.R. Matthews, C.E Wieman and E.A. Cornell, *Science* **269**, 198 (1995)

[2] C. J. Foot, in *Atomic Physics* (Oxford University Press, Oxford, 2005), pp. 182-208.

[3] M. W. Zwiernik. Ph.D. Thesis, Massachusetts Institute of Technology, 2006.